

## DYNAMICS AND CHAOS IN WAVY VORTEX FLOW

Alp Akonur<sup>1</sup> and Richard M. Lueptow<sup>2\*</sup>

<sup>1</sup>Department of Mechanical Engineering, Northwestern University, Evanston, IL, USA (currently at Baxter Healthcare Corporation, Round Lake, IL, USA)

<sup>2</sup>Department of Mechanical Engineering, Northwestern University, Evanston, IL, USA

\*Corresponding author: Richard M. Lueptow, r-lueptow@northwestern.edu

### Abstract

Dynamics of transport and mixing in a Couette-Taylor device was investigated by computationally tracking fluid particles using a three-dimensional, three-component experimental velocity field determined with recent particle image velocimetry (PIV) measurements at conditions well above transition to wavy vortex flow. Results indicate enhanced mixing due to increased stretching and folding in all directions. This results in very effective axial dispersion of fluid particles. Waviness and increasing vortex strength results in enhanced axial dispersion as the Reynolds number increases.

### Introduction

Couette-Taylor flow devices are used in applications where uniform mixing of a fluid is required [1-3]. Most of these devices operate under conditions where the outer cylinder is fixed and the inner cylinder is rotating. Numerous studies have been performed to understand the details of mixing in the wavy vortex flow regime, where most Couette-Taylor devices operate. Experiments have been aimed at obtaining parameters such as (i) the axial dispersion coefficient, (ii) the intercell mixing coefficient, and (iii) the intermixing coefficient [1, 4]. Moore and Cooney showed that the axial dispersion coefficient did not change with molecular diffusivity indicating that convection by vortical motion is much more important than molecular diffusion [1]. Ohmura et al. found that the intermixing coefficient increases with increasing waviness indicating the importance of the wavy motion of vortex cell boundaries and the fluid transport between vortices [4].

Theoretical studies have suffered from the absence of a reliable velocity field for wavy vortex flow, particularly well above the transition to wavy flow. Both a model velocity field and a theoretical velocity field for wavy cylindrical Couette flow have been used to evaluate the transport of fluid particles very near the transition from nonwavy to wavy vortices [5, 6]. The model of Rudolph et al. [7] was an attempt to consider conditions well above transition from nonwavy to wavy vortices, but their model was essentially a two-dimensional analog of three-dimensional wavy vortex flow based on the meridional plane measurements of Wereley and Lueptow [8]. Rudman used a computational model

to track fluid particles and evaluate the effective diffusion for wavy vortex flow [9]. In this paper, we track fluid particles in the full experimental three-dimensional velocity field obtained by Akonur and Lueptow [10], which is available at three different Reynolds numbers well above the transition from nonwavy to wavy vortex flow.

### Methods

Mixing in wavy vortex flow was investigated by tracking fluid particles, i.e. infinitesimally small particles with densities identical to that of the fluid. The equations  $dr/dt=v_r$ ,  $dz/dt=v_z$ , and  $d\theta/dt=v_\theta/r$  were integrated using a fourth order Runge-Kutta scheme. Validation of the integration and interpolation schemes was performed using a mathematically generated circular velocity field with a constant azimuthal velocity. After 370 revolutions the error in the calculated radial position of the particle compared to the exact solution was less than 0.01%.

The tracking of particle positions was based on a time-resolved, three-dimensional, three-component velocity field that was experimentally determined using PIV. The velocities in meridional (r-z) and latitudinal (r- $\theta$ ) planes were obtained independently [8], [10] by calculating the spatial cross-correlation of pairs of digital images of the flow seeded with micron size tracer particles that were illuminated by a laser light sheet in r-z and r- $\theta$  planes, respectively. The cross-correlation provided average displacements and therefore velocities of tracer particles. Then, the two sets of independent measurements obtained in r-z and r- $\theta$  planes were matched, as depicted in Fig. 1, based on the common radial velocity  $v_r$ , which was measured in both cases.

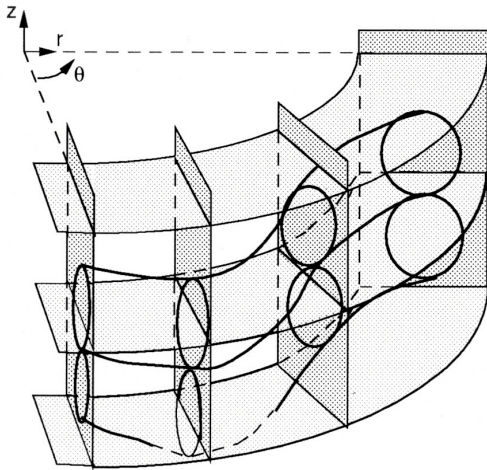


Fig. 1. Sketch of the PIV measurement planes. Measurements in meridional ( $r$ - $z$ ) planes were matched to measurements in latitudinal ( $r$ - $\theta$ ) planes by shifting the planes to minimize the difference in the radial velocity, which was measured in both cases.

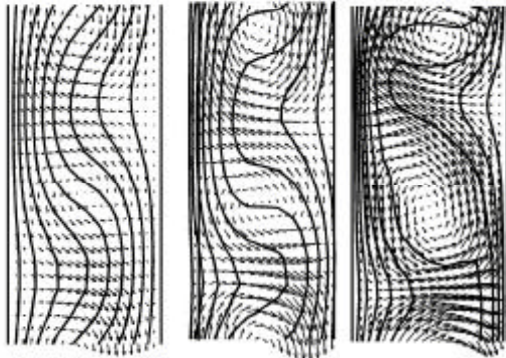


Fig. 2. Radial ( $v_r$ ) and axial ( $v_z$ ) velocity vectors in a meridional plane overlaid with azimuthal velocity contours shown at the same approximate phase of the azimuthal wave. (a)  $\epsilon=0.28$ , (b)  $\epsilon=1.48$ , (c)  $\epsilon=5.03$ , where  $\epsilon=Re/Re_{cr}-1$ . The azimuthal velocity contours are equally spaced between 0 at the outer cylinder (right side) and  $1.0 r_i \Omega$  at the inner cylinder (left side).

Fig. 2 shows the azimuthal velocity contours overlaying the radial and axial velocity vectors for three different Reynolds numbers,  $Re=r_i \Omega d/\nu$ , increasing from left to right, where  $r_i$  is the radius of the inner cylinder,  $\Omega$  is the rotational speed,  $d$  is the gap between the cylinders, and  $\nu$  is the kinematic viscosity. Increasing radial and axial azimuthal momentum transport related to increasing vortical strength and fluid transfer between neighbouring

vortices is responsible for the deformation of the azimuthal velocity contours. In addition, radial and axial motion of vortex centers is also evident when a time sequence of images like those in Fig. 2 is considered.

## Results

The dynamics of mixing in a Couette-Taylor device can be best understood by visualizing the deformation of an axial line of particles. In Fig. 3, initial lines of 2,000 particles starting from three different radial positions,  $(r-r_i)/d=0.25, 0.50, 0.75$ , are shown for a fixed azimuthal initial position corresponding to the meridional plane in which the azimuthal wave is at its rightmost axial position for  $\epsilon=1.48$ . The lines of particles initially extend a distance of  $2\lambda$ , where  $\lambda$  is the axial wavelength, approximately from the center of one clockwise (CW) vortex to another. The particle positions are superposed at times  $t=0, 0.5T, 1.0T$ , where  $T$  is the period of the azimuthal traveling wave. The top line represents the outer cylinder (OC), and the bottom line represents the inner cylinder (IC).

Clearly, common to all initial radial starting positions, axial lines of particles are subject to extensive stretching and folding, characteristic of mixing in chaotic flow. In the top frame of Fig. 3, a relatively thin tongue is enclosed by a similar larger tongue at  $T=1.0$  indicating self-similar structures of folded elements as time evolves. The existence of horseshoe-shaped structures also indicates effective stretching and folding implying chaotic mixing.

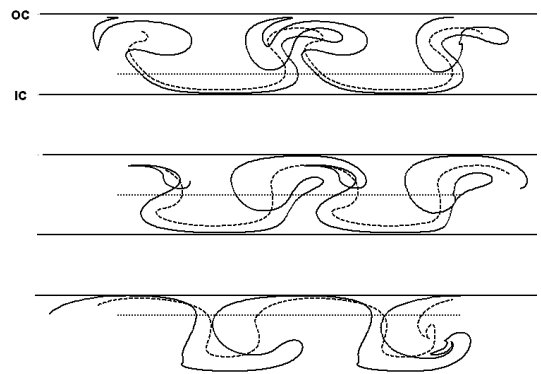


Fig. 3. Deformation of the axial line of 2,000 particles initially about  $2\lambda$  long initially located at  $(r-r_i)/d=0.25$  (top), 0.5 (middle), 0.75 (bottom) for  $t=0$  (dotted),  $0.5T$  (dashed), and  $1.0T$  (solid) viewed in a meridional plane for  $\epsilon=1.48$ .

The degree of stretching and folding increases with decreasing initial radial position, i.e. particles

starting closer to the inner cylinder, and with increasing Reynolds number  $\epsilon$  (not shown). The dependence of folding and stretching on  $\epsilon$  is somewhat surprising since it has been shown that fluid transport between vortices is greater for  $\epsilon=1.48$  than that for  $\epsilon=0.28$  and  $\epsilon=5.03$  [8]. However, the strength of the vortical motion increases with increasing  $\epsilon$ . Apparently, this increase in vortex strength is more important than transport between vortices in determining the degree of mixing and folding.

The dependence of chaotic folding and stretching on radial position can be explained by the increased azimuthal velocity close to the inner cylinder. Since the azimuthal velocity near the inner cylinder is greater than the velocity of the azimuthal waves, fluid particles near the inner cylinder are carried past more wavy structures than particles near the outer cylinder where the azimuthal velocity is less than that of the azimuthal traveling waves. This provides an axial line of particles initially near the inner cylinder more opportunity for folding and stretching than particles initially near the outer cylinder.

It is also helpful to consider axial dispersion of particles over time. Fig. 4 shows the positions of 1,250 particles initially distributed along a single axial line  $\lambda$  long (2 vortices) at the middle of the annulus for 2T, 4T, 6T, and 8T at  $\epsilon=1.48$ . In addition to the very quick inter-vortex mixing, it is evident that by 8T, particles have penetrated eight vortices via intra-vortex mixing. Estimates of the effective axial dispersion indicate that this effect increases with increasing Reynolds number.

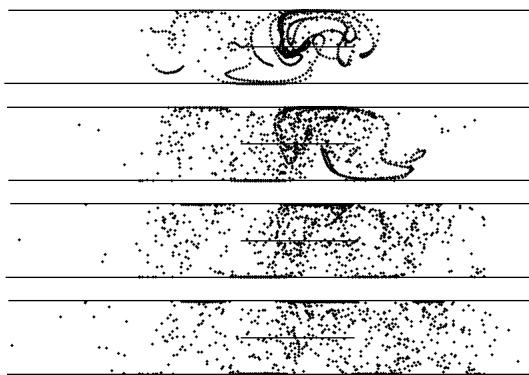


Figure 4. Positions of 1,250 particles initially on an axial line at  $(r-r_i)/d=0.5$  after 2T, 4T, 6T, and 8T for  $\epsilon=1.48$  viewed in a meridional plane.

## Conclusions

The experimentally obtained three-dimensional flow field for wavy cylindrical Couette flow was used to track particles for several Reynolds numbers to investigate the mixing characteristics of the flow field. At increasing Reynolds numbers, the particles experience chaotic mixing causing them to disperse axially as well as radially due to increasing vortical motion and transfer of fluid between vortices.

## Acknowledgements

This work was funded by the National Science Foundation.

## References

- [1] Moore, C.M.V., and Cooney, C.L., 1995, "Axial dispersion in Taylor-Couette flow", *AIChE J.*, 41:723-727.
- [2] Campero, R.J., and Vigil, R.D., 1997, "Axial dispersion during low Reynolds number Taylor-Couette flow: intra-vortex mixing effects", *Chem. Eng. Sci.*, 52:3303-3310.
- [3] Lee, S., and Lueptow, R.M., 2001, "Rotating reverse osmosis: a dynamic model for flux and rejection", *J. Memb. Sci.* to appear (2001).
- [4] Ohmura, N., Kataoka, K., Shibata, Y., and Makino, T., 1997, "Effective mass diffusion over cell boundaries in Taylor-Couette flow system", *Chem. Eng. Sci.*, 52: 1757-1765.
- [5] Broomhead, D.S., and Ryrie, S.C., 1988, "Particle paths in wavy vortices", *Nonlinearity*, 1: 409-434.
- [6] Ashwin, P., and King, G.P., 1997, "A study of particle paths in non-axisymmetric Taylor-Couette flows", *J. Fluid Mech.*, 338: 341-362.
- [7] Rudolph, M., Shinbrot, T., and Lueptow, R.M., 1998, "A model of mixing and transport in wavy Taylor-Couette flow", *Physica D*, 121: 163-174.
- [8] Wereley, S.T., and Lueptow, R.M., 1998, "Spatio-temporal character of supercritical circular Couette flow", *J. Fluid Mech.*, 364: 59-80.
- [9] Rudman, M., 1998, "Mixing and particle dispersion in the wavy vortex regime of Taylor-Couette flow", *AIChE J.*, 44: 1015-1026
- [10] Akonur, A., Lueptow, R.M., 2001, "Three-dimensional velocity field for nonwavy and wavy Taylor-Couette flow", submitted to *J. Fluid Mech.*